



Strengthening Effect of Mn and Si Powders on Laser Penetration Welding Joints between Dual Phase Steel and Aluminum Alloy

Dianwu Zhou*, Jinshui Liu, Yuanzhi Lu and Shaohua Xu

State Key Laboratory of Advanced Design and Manufacturing for Vehicle Body, Hunan University, China

Abstract

Laser penetration welding of DP590 dual phase steel to 6016 aluminum alloy was studied in steel-on-aluminum overlap configuration with the addition of Mn and Si powders. Microstructure and mechanical properties of joints were examined. Results reveal that the average tensile-shear strength of Si-added joint is 3.84% higher than that of Mn-added joint, and the strength of both joints exceeds that of no-added joint. Composition and thickness of IMCs both play a vital role in strengthening the joints, but strengthening effect on Si-added joint is better than that on Mn-added joint.

Keywords

Laser penetration welding, Microstructure, Mechanical properties

Introduction

In recent years, the demand for fuel consumption and protecting environment in automotive industry leads to the increased interest in reducing vehicle weight [1]. Joining steel to aluminum has been considered as one of the most effective measures [2-5]. However, it is very difficult for welding of steel and aluminum due to the formation of brittle intermetallic compounds (IMCs). Laser welding can shorten the metallurgical reaction time with high welding speed. In other words, the formation of IMCs can be suppressed. Sierra, et al. [5] suggested a steel-on-aluminum overlap configuration, and thought the formation of IMCs is suppressed by controlling steel penetration in aluminum. Later, many researchers have been stepping up efforts to join steel to aluminum by using this method [6-8]. However, these investigations only optimized the joint properties with respect to process parameter or heat source. Improving the metallurgical reaction is an effective way of enhancing the joint properties. Usually, adding an interlayer can improve the metallurgical reaction of molten pool for laser welding [9-12]. In this paper, laser penetration welding of DP590

dual phase steel to 6016 aluminum alloy was studied in steel-on-aluminum overlap configuration with the addition of Mn and Si powders. Microstructure and mechanical properties of joints were examined. The influence of adding Mn and Si powders on the joint properties was discussed.

Materials and Methods

DP590 dual phase steel ($100 \times 30 \times 1.4$ mm, C \leq 0.15, Si \leq 0.60, Mn \leq 2.50, S \leq 0.015, P \leq 0.040 and Fe = Bal. (wt.)) and 6016 aluminum alloy ($100 \times 30 \times 1.2$ mm, Si = 1.0-1.5, Mg = 0.25-0.6, Fe \leq 0.5, Mn \leq 0.2, Cu \leq 0.2 and Al = Bal.(wt.)) plates were prepared for deep penetration laser welding. Mn or Si powder, with 99.9% purity, 75- μ m average size, and 0.1 mm thick was added between dual phase steel and aluminum alloy as interlayer. A YLS-4000-CL fiber laser system with maximum output power of 4000 W was used. The focus point with a diameter of 0.4 mm was on the upper surface of dual phase steel in the steel-on-aluminum overlap configuration. Deep penetration laser welding test with Mn or Si powder was carried out to obtain a good weld not only a weld with

*Corresponding author: Dianwu Zhou, State Key Laboratory of Advanced Design and Manufacturing for Vehicle Body, Hunan University, Changsha 410082, China, Tel: +86-13017297124, Fax: +86-7318821483, E-mail: ZDWe_mail@126.com

Received: May 05, 2018; Accepted: June 07, 2018; Published: June 09, 2018

Copyright: © 2018 Zhou D, et al. This is an open-access article distributed under the terms of the Creative Commons Attribution License, which permits unrestricted use, distribution, and reproduction in any medium, provided the original author and source are credited.

Citation: Zhou D, Liu J, Lu Y, Xu S (2018) Strengthening Effect of Mn and Si Powders on Laser Penetration Welding Joints between Dual Phase Steel and Aluminum Alloy. Int J Metall Met Phys 3:014

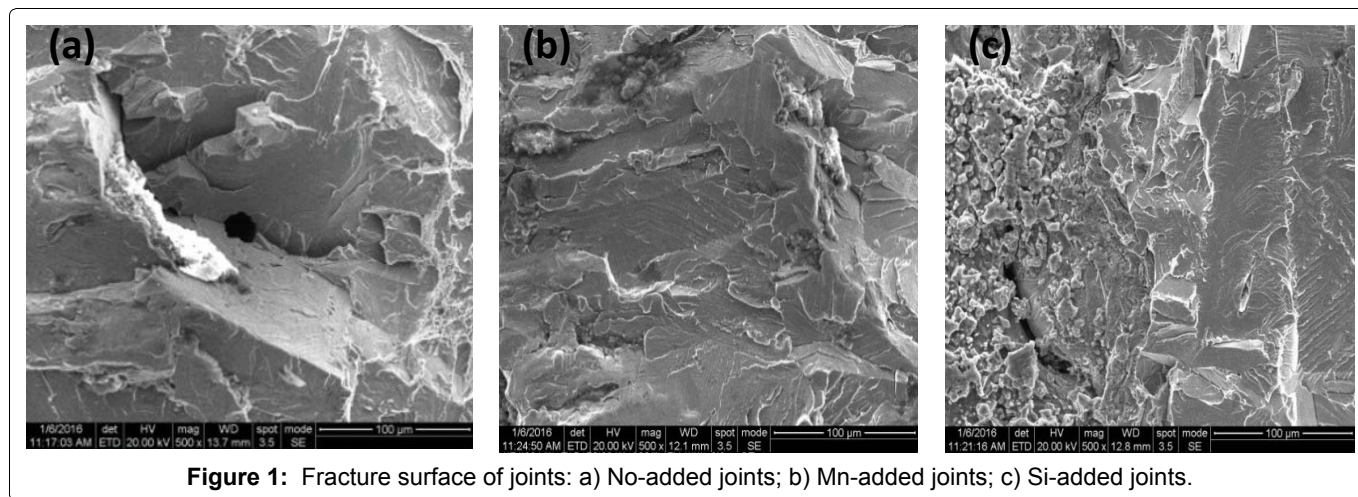


Figure 1: Fracture surface of joints: a) No-added joints; b) Mn-added joints; c) Si-added joints.

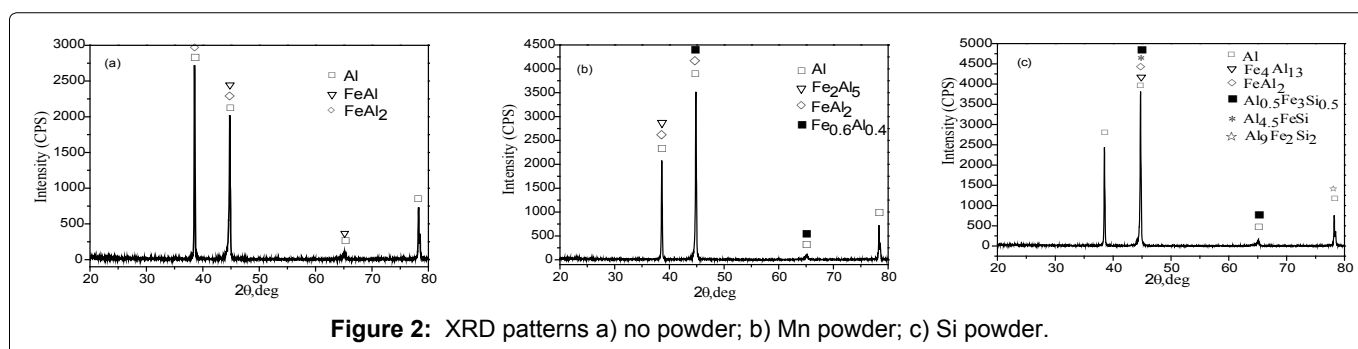


Figure 2: XRD patterns a) no powder; b) Mn powder; c) Si powder.

sufficient penetration but also an acceptable weld surface. The optimal process parameters were determined as follows: Welding power is 2000 W, welding speed is 50 mm/s, the defocus distance is +2 mm, and flow rate of Ar protective gas is 15 L/min. The process parameters of adding powder were the same as that of no powder in order to identify the effect of adding powder on microstructure and properties of the welded.

The specimens were prepared across the weld by wire-cutting for microstructure observations. The cross-sections were grinded by standard procedures. Microstructure, fracture morphology and interface elements distribution were performed by FEI Quanta 200 scanning electron microscopy equipped with spectrometer (EDS) probe. Crystalline phase of joints were identified by X-ray diffraction (XRD). Both tensile and shear forces are applied to the interface during test due to non-symmetric configuration of the tensile test samples. Hence, in the current study, the joint strength is given in N/mm (failure strength divided by the width of tested specimen) since it is difficult to separate tensile and shear stress. According to the BS EN 1002-1:2001 standard, the tensile-shear tests are operated at room temperature using INSTRON 5569 at a crosshead speed of 1 mm/min. Average joint strength is calculated from three tensile specimens.

Results and Discussion

The current experiment shows that the tensile-shear

strength of Si-added joint which is 108 N/mm is 3.84% higher than that of Mn-added one that is 104 N/mm, and the strength of both joints exceeds that of no-added joint. Further inspection is performed on the fracture surfaces shown in Figure 1. It is found that the fracture surface of no-added or Mn-added joint shows a river shape pattern, which shows typical brittle fracture features. However, the fracture surface of Si-added joint displays micro-scale toughening nest and a small amount of inclusions, which is quasi-cleavage fracture, suggesting that the joint owns certain plasticity.

XRD and EDS were performed to understand the influence of adding powder on the joint properties. XRD patterns with/without powders is shown in Figure 2. It can be seen that some IMCs are formed, such as FeAl, FeAl₂, Fe₂Al₅, Fe₃Al₂, FeAl₃, Al_{4.5}FeSi, Al_{0.5}Fe₃Si_{0.5} and Al₉Fe₂Si₂. Table 1 shows that the EDS results at the A-V zones in Figure 3. As far as no-added joint is concerned, some isolated particles are distributed at the interface zone, a severe interfacial reaction occurs, and IMCs with thickness of about 20 μm are formed between the fusion zone and aluminum alloy. At B zone, the Al content is less, mainly for Fe. At C and D zone, the Fe/Al ratio is very close to 1:1, 1:2, respectively. Thus, FeAl and FeAl₂ may be formed at C and D zones. In the case of adding Mn powder, as compared to no-added joint, micro-structural morphologies seem to be unchanged, but aluminum molten pool seems to be expanded, and thick-

ness of IMCs is about 12 μm. At G, H and I zones, the Fe/Al ratio are very close to 3:2, 1:2, 2:5, respectively. It is confirmed that the layer at G-H zone are composed of Fe₃Al₂, FeAl₂ and Fe₂Al₅. From the view of Si-added joint, it is evident that welding penetration depth increases compared with that of no-added joint, and thickness of IMCs is about 9-10 μm. At P, Q and R zones, the Fe/Al ratio are very close to 1:1, 1:2, 1:3, respectively. Thus, it is thought that the layer at P-Q zone are composed of FeAl, FeAl₂ and FeAl₃.

To investigate elemental distribution of joints with/without powders, EDS linear scanning was performed, as shown in Figure 4. It can be seen that the contents of Fe and Al both change drastically in steel molten pool (Figure 4b and Figure 4c). This indicates that liquid Al rise and mix into the fusion zone with no powder. However, in the case of adding Mn powder, it is not obvious for the change of Fe and Al contents in steel molten pool (Figure 4e), and the distribution width of Al element in aluminum molten pool increases compared with that of no powder (Figure 4f). When Si powder is added, the mixture of Fe and Al is both found in upper and lower molten pool (Figure 4h and Figure 4i), which indicates that the liquidity and metallurgical reaction of molten pool can be improved.

The addition of Mn and Si powders into lap joint of

Table 1: EDS results A to V zones in Figure 1 (at.pct).

Element/zone	Fe	Al	Mn	Si	Phase
A	70.1	27.59	1.32	0.99	Unknown
B	83.72	13.31	1.77	1.21	Fe-rich
C	43.52	55.28	0.93	0.27	FeAl
D	36.19	62.81	0.74	0.25	FeAl ₂
E	83.7	9.16	1.67	1.87	Fe-rich
F	73.96	22.34	2.83	0.88	Fe-rich
G	58.49	38.54	1.99	0.99	Fe ₃ Al ₂
H	35.83	62.5	1.26	0.41	FeAl ₂
I	27.24	71.76	0.84	0.16	Fe ₂ Al ₅
J	18.39	80.68	0.76	0.18	Al-rich
K	81.53	14.4	2.51	1.55	Fe-rich
L	45.87	52.13	1.39	0.61	Fe ₃ Al ₂ , FeAl ₂
M	79.72	16.97	2.29	1.01	Fe-rich
N	87.78	9.36	2.27	1.2	Fe-rich
O	25.33	73.45	1.04	0.19	FeAl, FeAl ₂
P	54.23	43.82	1.08	0.86	FeAl
Q	34.88	63.72	0.89	0.51	FeAl ₂
R	22.94	76.63	0.43	0	FeAl ₃
S	90.1	5.97	1.94	1.99	Fe-rich
T	70.3	26.26	1.57	1.8	Fe-rich
U	27.15	68.49	0.62	3.74	FeAl, FeAl ₂
V	58.66	38.37	1.61	1.35	Fe ₃ Al ₂

DP590 dual phase steel to 6016 aluminum alloy improve tensile-shear strength of joints. It is well known that mechanical properties of joints are closely related to mor-

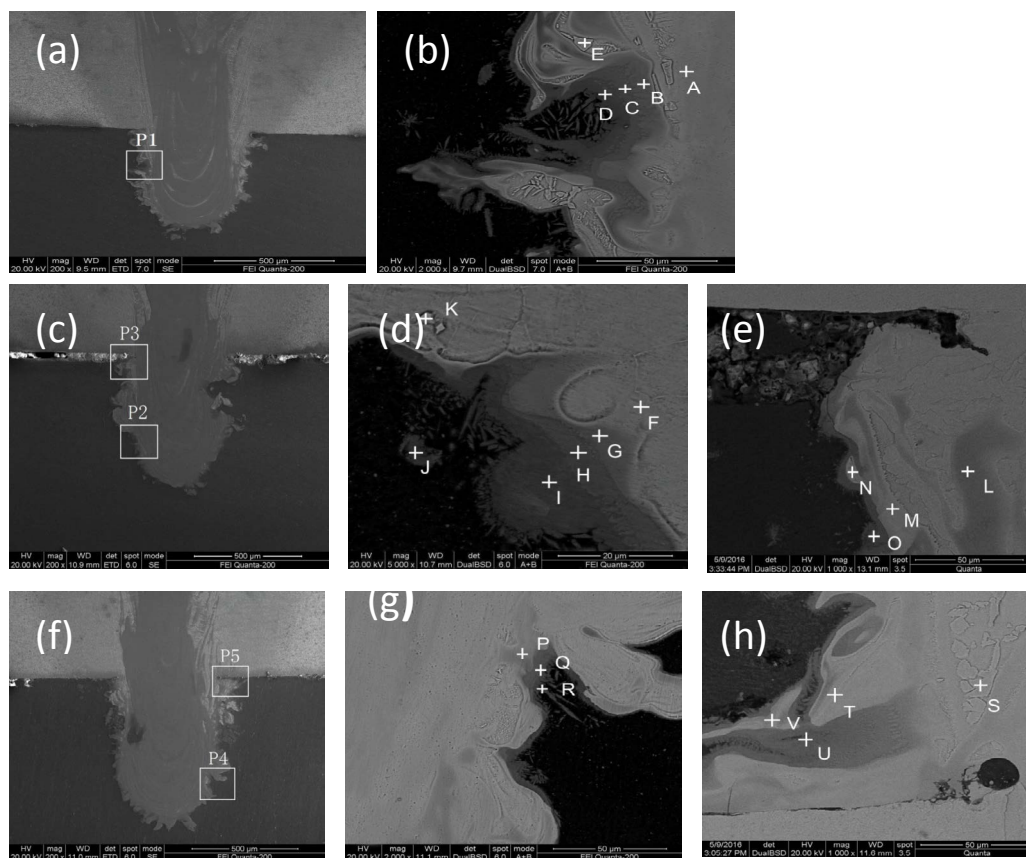


Figure 3: Microstructure of joints: (a), (c) and (f) cross-section of no, Mn and Si powders, (b), (d), (e) (g) and (h) magnification of P1 in Figure 3a, P2, P3 in Figure 3c, P4, P5 zone in Figure 3f.

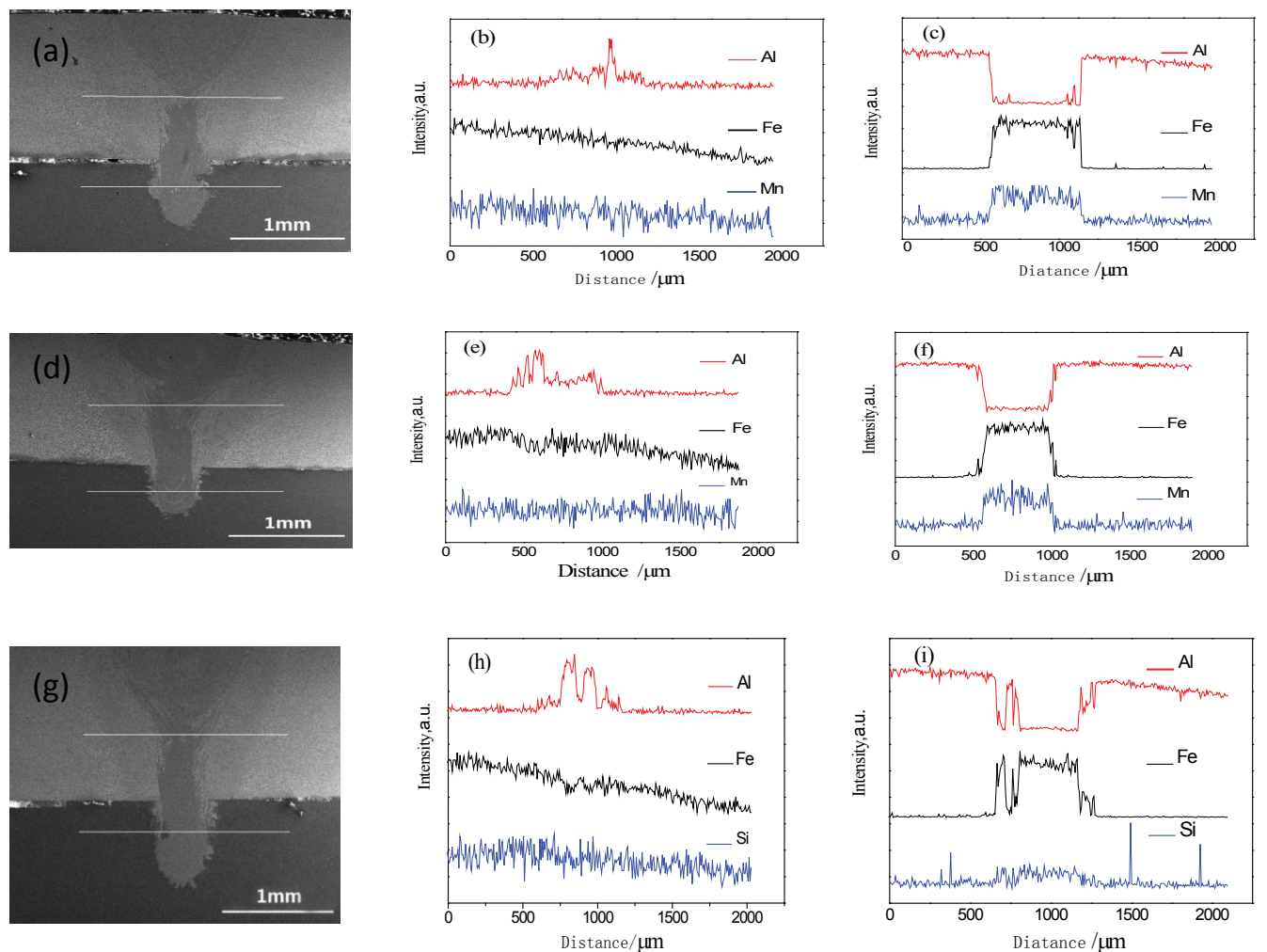


Figure 4: EDS liner scanning of the elements distributions of joints: (a), (d) and (g) scanning position of no, Mn and Si powders, (b), (e) and (h) scanning line I, (c), (f) and (i) scanning line II, respectively.

phology and distribution of microstructures, especially to that of IMCs phase in the joints. In the present study, the decreased IMCs thickness is found in both Mn- and Si-added joints. This indicates the formation of brittle IMCs can be suppressed effectively, which is benefit for the improved properties of the joints. In addition, the blockage effect of Mn powder as interlayer can be seen in Figure 3 and Figure 4, because EDS analysis of IMCs in the joint indicates that Mn is not involved in metallurgical reaction with Fe or Al. Nevertheless, small amount of liquid Al is mixed into steel molten pool, which leads to the increased weld width in aluminum molten pool. Thus, transverse area increase in jointing steel to aluminum, which is significance for the improved tensile-shear strength of joints [13]. As far as adding Si powder is concerned, it is not the case, the regulation effect of Si powder can be seen in Figure 3 and Figure 4, and the enhancement of the joint properties benefits from improvement of metallurgical reaction. The FeAl phase transforms into $Al_{4.5}FeSi$, $Al_{0.5}Fe_3Si_{0.5}$ and $Al_9Fe_2Si_2$ after Si powder is added. The phases $Al_{4.5}FeSi$ and $Al_9Fe_2Si_2$ are similar to Fe_2Al_5 with regard to crystal structure, but Fe

atom in lattice is replaced for Si. The phase $Al_{0.5}Fe_3Si_{0.5}$ is similar to Fe_3Al , but Al atom in lattice is replaced for Si. According to the Fe-Al phase diagram, IMCs of Fe_3Al , FeAl, $FeAl_2$, Fe_2Al_5 and $FeAl_3$ are easily formed. Among these, Fe-rich IMCs are recognized as ductile and tough phases while Al-rich IMCs are hard and brittle phases [6,7]. Thus, formation of the IMC $Al_{0.5}Fe_3Si_{0.5}$ with ductility and toughness is an important reason of enhancing mechanical properties of the joint with Si powder.

Conclusion

In summary, DP590 dual phase steel and 6016 aluminum alloy is successfully lap joined by laser penetration welding technique with the addition of Mn and Si powders. The average tensile-shear strength of Mn-added and Si-added joints can exceed that of no-added joint. Although strengthening effect of the joint is similar, strengthening mechanism is dissimilar a little. Composition and thickness of IMCs both played a vital role in strengthening the joints, and the addition of Si powder into the joints is superior to that of Mn powder in tensile-shear strength. As far as adding Si powder is con-

cerned, the enhancement of the joint properties benefits from improvement of metallurgical reaction.

Acknowledgment

The work was supported by National Natural Science Foundation of China (Grant No. 51674112, 51774125) and National Key Research and Development Project of China (Grant No. 2018YFB1107905).

References

1. Sierra G, Wattrisse B, Bordreuil C (2008) Structural analysis of steel to aluminum welded overlap joint by digital image correlation. *Exp Mech* 48: 212-223.
2. Fan J, Thomy C, Vollertsen F (2011) Effect of thermal cycle on the formation of intermetallic compounds in laser welding of aluminum-steel overlap joints. *Physics Procedia* 12: 134-141.
3. Dharmendra C, Rao K, Wilden J, Reich S (2011) Study on laser welding-brazing of zinc coated steel to aluminum alloy with a zinc based filler. *Mater Sci Eng A* 528: 1497-1503.
4. Ma J, Harooni M, Carlson B, Kovacevic R (2014) Dissimilar joining of galvanized high-strength steel to aluminum alloy in a zero-gap lap joint configuration by two-pass laser welding. *Mater Design* 58: 390-401.
5. Sierra G, Peyre P, Deschaux-Beaume F, Stuart D, Fras G (2007) Steel to aluminium key-hole laser welding. *Mater Sci Eng A* 447: 197-208.
6. Torkamany MJ, Tahamtan S, Sabbaghzadeh J (2010) Dissimilar welding of carbon steel to 5754 aluminum alloy by Nd: YAG pulsed laser. *Mater Design* 31: 458-465.
7. Chen HC, Pinkerton AJ, Li L, Liu Z, Mistry AT (2011) Gap-free fibre laser welding of Zn-coated steel on Al alloy for lightweight automotive applications. *Mater Design* 32: 495-504.
8. Shi Y, Zhang H, Takehiro W, Tang J (2010) CW/PW dual-beam YAG laser welding of steel/aluminum alloy sheets. *Optics and Lasers in Engineering* 48: 732-736.
9. Zhou DW, Xu SH, Peng L, Liu JS (2016) Laser lap welding quality of steel/aluminum dissimilar metal joint and its electronic simulations. *The International Journal of Advanced Manufacturing Technology* 86: 2231-2242.
10. Chen SH, Huang JH, Ma K, Zhao XK, Vivek A (2014) Microstructures and mechanical properties of laser penetration welding joint with/without Ni-foil in an overlap steel-on-aluminum configuration. *Metallurgical and Materials Transactions A* 45: 3064-3073.
11. Chen SH, Huang JH, Ma K, Zhang H, Zhao XK (2012) Influence of a Ni-foil interlayer on Fe/Al dissimilar joint by laser penetration welding. *Mater Lett* 79: 296-299.
12. Yang XD, Shi Y, Liu J (2014) Effect of Cu foil on laser butt welding quality of aluminum/steel dissimilar metals joint. *Journal of Mechanical Engineering* 50: 143-149.
13. Liu M, Jiang JB (2009) The effect of adhesive layer on variable polarity plasma arc weld bonding process of magnesium alloy. *Journal of Materials Process Technology* 209: 2864-2870.